

Exploring the best way for UAV visual localization under Low-altitude Multi-view Observation Condition: a Benchmark

Yibin Ye¹, Xichao Teng¹, Shuo Chen¹, Zhang Li^{1,✉}, Leqi Liu¹, Qifeng Yu¹, Tao Tan²

¹National University of Defense Technology, Changsha, China zhangli_nudt@163.com

²Macao Polytechnic University, Macao, China

Abstract

*Absolute Visual Localization (AVL) enables Unmanned Aerial Vehicle (UAV) to determine its position in GNSS-denied environments by establishing geometric relationships between UAV images and geo-tagged reference maps. While many previous works have achieved AVL with image retrieval and matching techniques, research in low-altitude multi-view scenarios still remains limited. **Low-altitude Multi-view** condition presents greater challenges due to extreme viewpoint changes. To explore the best UAV AVL approach in such condition, we proposed this benchmark. Firstly, a large-scale Low-altitude Multi-view dataset called **AnyVisLoc** was constructed. This dataset includes 18,000 images captured at multiple scenes and altitudes, along with 2.5D reference maps containing aerial photogrammetry maps and historical satellite maps. Secondly, a **unified framework** was proposed to integrate the state-of-the-art AVL approaches and comprehensively test their performance. The best combined method was chosen as the **baseline** and the key factors that influencing localization accuracy are thoroughly analyzed based on it. This baseline achieved a **74.1%** localization accuracy within 5m under Low-altitude, Multi-view conditions. In addition, a novel retrieval metric called **PDM@K** was introduced to better align with the characteristics of the UAV AVL task. Overall, this benchmark revealed the challenges of Low-altitude, Multi-view UAV AVL and provided valuable guidance for future research. The dataset and codes are available at <https://github.com/UAV-AVL/Benchmark>*

1. Introduction

In recent years, Unmanned Aerial Vehicles (UAVs) are widely used in various fields like precision agriculture, emergency response, and transportation, etc [11]. These outdoor drones generally rely on Global Navigation Satellite System (GNSS) and inertial navigation system (INS) for localization. However, GNSS signals are prone to dropout

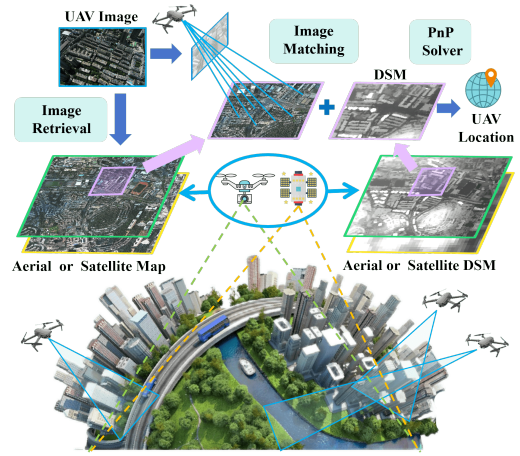


Figure 1. **Benchmark Overview.** This benchmark focuses on UAV visual localization under low-altitude multi-view observation condition using the 2.5D aerial or satellite reference maps. The visual localization is mainly achieved via a unified framework combining image retrieval, image matching, and PnP problem solving.

and jamming [49], while INS suffers from drifting over time [22]. Consequently, there is a growing interest in visual localization as a temporary alternative [7, 13, 22, 23].

Current UAV visual localization research can be primarily categorized into relative visual localization (RVL) and absolute visual localization (AVL) [10]. RVL approaches, such as Simultaneous Localization and Mapping (SLAM) [6], are commonly used for indoor robot navigation through frame-to-frame matching [7]. While RVL methods do not require geo-tagged maps, they also suffer from drift¹. In contrast, AVL approaches, which involve matching UAV images with geo-tagged reference maps, have inherent immunity to drift and are the focus of this paper.

To the best of our knowledge, most previous studies focused on nadir-view based AVL [5, 23, 32, 35, 44]. Besides, the regions that being imaged for AVL are usually with sig-

¹Note that Loop closure can somewhat improve global localization accuracy, but it is hard to achieve for long-distance outdoor flights [11].

nificant lower altitude than UAV flight altitude [52]. In these scenarios, the observed regions are often assumed as planar. Therefore, one can use homography or sRt model to estimate the transformation between UAV images and geo-tagged reference maps [38]. However, this ideal assumption does not apply to UAV visual localization under **Low-altitude** ($< 300m^2$) and **Multi-view** (with pitch angles³ ranging from 20° to 90°) observation condition. The significant viewpoint changes at low altitude introduce severe nonlinear transformation between UAV images and reference maps and present greater challenges for visual localization [50, 51]. How current AVL methods perform in these challenging scenarios is still unclear. Meanwhile, no public available datasets could be used to comprehensively benchmark current AVL methods. To fill this gap, we constructed a new dataset called AnyVisLoc and conducted extensive experiments on this dataset to evaluate all UAV AVL methods under Low-altitude Multi-view condition. Overall, our contributions are as follows:

- The **first large-scale Low-altitude Multi-view** dataset called **AnyVisLoc** was proposed. This dataset contains 18,000 UAV images captured at multiple scenes and altitudes, along with two types of 2.5D reference maps including aerial photogrammetry maps and satellite maps.
- A **unified framework** was introduced to integrate the state-of-the-art AVL approaches and thoroughly test their performance. The best combined method was chosen as the **baseline** and the key factors that influencing baseline accuracy are thoroughly discussed, including the type of reference maps, different pitch angles and the noise in prior information.
- A novel retrieval metric called **PDM@K** was designed to bridge the relationship between image retrieval accuracy and final localization accuracy. Compare to other metrics like Recall@K and SDM@K, PDM@K aligns more closely with the characteristics of the UAV AVL task.

2. Related Work

Image-Level Retrieval can be used to estimate the rough position of UAV image on the reference map [8, 50]. These approaches includes Template Matching (TM) [40] and Visual Geo-localization (VG) [4] methods. All these methods rely on constructing feature patterns to measure similarity between drone (query) and reference (gallery) images. The similarity metrics commonly used for TM (e.g., NCC [40], MI [52]) are not invariant to viewpoint differences, making them less suitable for low-altitude, multi-view observation condition. In contrast, deep learning-based VG methods are more adaptable to changes in viewpoint [56]. NetVLAD [2] is a widely adopted VG baseline. In the field

²According to relevant regulations, civilian UAVs are not permitted to fly above 300 meters [1]

³the angle between the optical axis and the horizontal plane

of drone-to-satellite retrieval, several studies concentrate on refining network architectures [27, 36, 42]. For instance, MCCG [36] incorporates a cross-dimensional interaction module and a multi-classifier structure to construct comprehensive feature representations. Additionally, some efforts are dedicated to enhancing training and sampling strategies [12, 15, 45, 47]. For example, Sample4Geo [15] employs InfoNCE loss to increase negative samples for contrastive learning within one batch. Meanwhile, CAMP [45] introduces comparisons between different scenes from the same imaging platform within the same training batch, thereby increasing the number of negative samples for contrast.

Pixel-Level Image Matching first establishes feature point correspondences between UAV images and reference map, subsequently solving the PnP problem to determine the UAV’s location [10, 21]. Pixel-level image matching, which comprises sparse and dense approaches [31], always achieve higher precision than image-level retrieval. The typical sparse approaches involve keypoint detection and keypoint matching steps. Traditional keypoint detectors like SIFT [30], SURF [3], and ORB [6] are widely used in sparse matching but are sensitive to large viewpoint differences. The rise of deep learning has brought learning-based detectors and descriptors into the mainstream to cope with viewpoint changes [14, 16, 33, 54]. Another line of sparse approaches focus on learning-based global relationship modeling among keypoints, such as SuperGlue[34], Lightglue [28] and Omniglue [25]. Dense approaches [17–19, 39] avoid keypoint detection and directly find dense correspondences between images, leading to significant improvements over sparse methods but with lower efficiency. Therefore, there is growing interest in creating lightweight and high-precision matching techniques [26, 31, 33, 43].

UAV Visual Localization Dataset. As summarized in Tab. 1, most current UAV datasets focus on nadir-view and lack multi-view coverage [13, 21, 32, 48]. Some datasets are restricted to specific scenes (e.g., urban [13] or wilderness [21] areas). Some datasets use synthetic data (e.g., Google Map Studio[55]) that do not fit the real application requirement. Although some recent geo-localization datasets include multi-view UAV images [55, 56], they often lack ground truth for UAV positions and continuous geographical coverage, which is not suitable for precise AVL.

Regarding reference maps, most datasets currently only have 2D satellite images and lack high-precision digital surface models (DSM) map[48]. Open-source like ALOS DSM $30m^4$ and NASADEM $30m^5$ have relatively low resolutions and do not meet the precise AVL needs under low-altitude multi-view observation condition.

To the best of our knowledge, none of the existing datasets simultaneously provide aerial reference map and

⁴https://www.eorc.jaxa.jp/ALOS/en/dataset/aw3d30/aw3d30_e.htm

⁵<https://www.earthdata.nasa.gov>

Table 1. UAV AVL datasets Comparison

Name	Year	UAV data	UAV Types	UAV Location	2D Reference	DSM	Flight Altitude	Observation	Scenes	Temporal
ATM[32]	2021	Real-scenes	1	✓	Aerial	×	unknown	Nadir-view	Urban	Multiple
University-1652[55]	2021	Synthetic	-	×	Satellite	×	121.5m to 256m	Multi-view	Buildings	-
Wildnav[21]	2022	Synthetic	-	✓	Satellite	×	unknown	Nadir-view	Wilderness	-
VPAIR[35]	2022	Real-scenes	1	✓	Satellite	✓	300m to 400m	Nadir-view	Multiple	-
SEUS-200[56]	2023	Real-scenes	-	×	Satellite	×	150/200/250/300m	Multi-view	Urban	-
DenseUAV[13]	2024	Real-scenes	1	✓	Satellite	×	80m/90m/100m	Nadir-view	Urban	Multiple
UAVD4L[46]	2024	Real-scenes	1	✓	Aerial	✓	50m to 151m	Multi-view	Urban	-
UAV-VisLoc[48]	2024	Real-scenes	unknown	✓	Satellite	×	400m to 2000m	Nadir-view	Multiple	Multiple
GTA-UAV[24]	2025	Synthetic	-	✓	Satellite	×	80m to 650m	Near nadir-view	Multiple	-
AnyVisLoc(Ours)	2025	Real-scenes	7	✓	Aerial & Satellite	✓	30m to 300m	Multi-view	Multiple	Multiple

satellite reference map of the same area. The work most similar to ours are [10, 38, 41, 50], although these literature explored the feasibility of AVL based on oblique-view, their test data lacked sufficient scene coverage, and the datasets and codes were not open-sourced yet.

3. AnyVisLoc Dataset

The UAV AVL accuracy is affected by various factors including viewing conditions (e.g., flight altitude, pitch angle, and field of view), flight environment (scene, weather, and illumination), and reference map characteristics (source, spatial resolution, and modality differences) [11, 50]. Our proposed AnyVisLoc dataset covers all possible factors for UAV AVL under Low-altitude Multi-view observation condition. This section gives a detailed description of it.

3.1. Data Acquisition and Processing

As shown in Fig. 3, we have collected a total of 18,000 UAV images using seven different types of DJI drones⁶ whose cameras vary in intrinsic parameters. The images were taken in 15 different cities across China under different weather (sunny, cloudy, rainy), seasons, and illuminations (day and night), covering 25 distinct regions. The imaging coverage area ranges from 10,000 m^2 to 9,000,000 m^2 . Each image is attached with camera intrinsic and extrinsic parameters, which can be used for UAV AVL as well as the ground truth.

Besides the UAV images, we provide two types of 2.5 D reference maps: **Aerial Photogrammetry Map** that is created by capturing images using the DJI Phantom 4 RTK drone and then using DJI Terra software⁷ to construct 2D orthophotos and DSM. **Satellite Map** that involves 2D historical images from Google Earth and ALOS 30m DSM. Both sets of 2.5D reference maps are geo-tagged and reprojected into the UTM coordinate system for geo-localization. More detailed information, such as latitude, longitude, and spatial resolution, is provided in the appendix.

⁶Mavic 2, Mavic 3, Mavic 3 Pro, Phantom 3, Phantom 4, Phantom 4 RTK, Mini 4 Pro

⁷<https://www.dji.com/downloads/products>

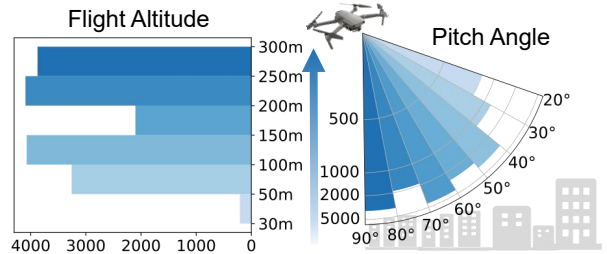


Figure 2. Pitch Angle and Flight Altitude Distribution.

3.2. Data Characteristics

- **Multi-altitude:** Our dataset covers low-altitude flight conditions from 30m to 300m (see Fig. 2 and Fig. 3).
 - **Multi-view:** Our dataset covers common used pitch angle of UAV imaging from 20° to 90° (see Fig. 2 and Fig. 3).
 - **Multi-scene:** Our dataset includes various scenes (see Fig. 3), such as dense urban areas (e.g., cities, towns, country), typical landmark scenes (e.g., playground, museums, church), natural scenes (e.g., farmland and mountains), and mixed scenes (e.g., universities and park).
 - **Multi-reference map:** Our dataset provides two types of 2.5D reference maps for different purposes (see Fig. 3). The aerial map with high spatial resolution can be used for high-precision localization but needs pre-aerial photogrammetry. The satellite map serves as an alternative when the aerial map is unavailable.
- Overall,** our dataset can facilitate a comprehensive evaluation of current UAV AVL methods under Low-altitude Multi-view observation condition.

3.3. Ground Truth Accuracy

For drone position accuracy, 40% of drone images were captured by DJI Phantom 4 RTK (RTK GPS, hover accuracy $\pm 0.1m$), and the rest used other DJI drones (standard GPS, hover accuracy $\pm 0.5m$)⁸. Regarding aerial photogrammetry map accuracy, we used highly overlapping aerial images and applied techniques including ground control point correction and global camera parameter optimiza-

⁸<https://www.dji.com/support/product/>

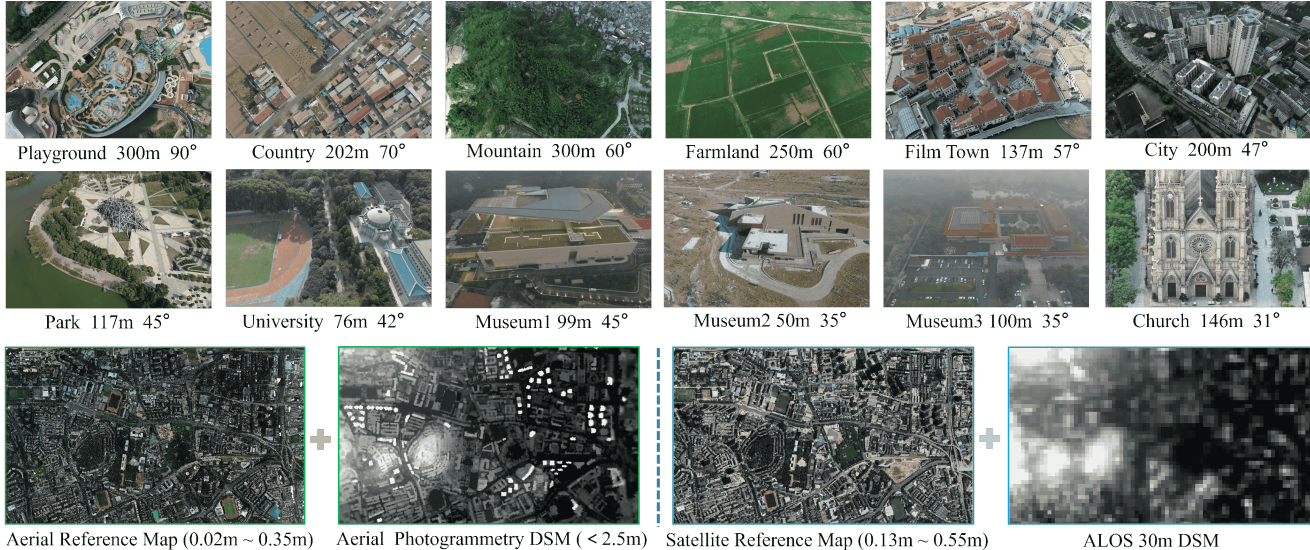


Figure 3. **Dataset Overview.** The AnyVisLoc dataset contains Multi-scene, Multi-altitude, and Multi-view UAV images taken in 15 cities across China, as well as aerial and satellite reference maps. Each UAV image shows its flight altitude and pitch angle below.

tion. After offline reconstruction, DJI Terra’s *quality reports* show an average reprojection error of 1.0 pixel and an average geo-registration error of 0.1 meters.

4. The Unified AVL Framework

Given a UAV image captured under Low-altitude, Multi-view observation condition, its field of view is within the reference map, but its exact position is unknown. Under such conditions, extreme viewpoint changes and a vast search space always result in image matching failures. Meanwhile, image retrieval can only provide a rough estimate of the current view’s position. Consequently, independently evaluating the performance of image retrieval or matching methods becomes challenging. Therefore, a unified framework is needed for fair and meaningful testing.

Framework Workflow: As shown in Fig. 1, the framework operates in a coarse-to-fine manner. Initially, image-level retrieval is used to estimate the rough position of current view, followed by pixel-level matching to obtain 2D-2D matched point pairs between the UAV image and the reference map. Subsequently, DSM data and the matching results are used to solve the PnP problem and determine the UAV’s geo-location. This framework can integrate with different reference maps and localization strategies.

Algorithm Integrated: The image retrieval approaches include template matching approaches like NCC[40] and MI[52], popular retrieval model like NetVLAD[2], and drone-to-satellite retrieval approaches such as CNN-based models⁹ and transformer-based models¹⁰. Matching tech-

niques include handcrafted SIFT[30], ORB[6] and learning-based sparse feature approaches¹¹ and (semi-)dense feature approaches¹². The PnP solver is P3P+RANSAC[20].

Additionally, we compare four localization strategies: (a) Matching the Top-1 retrieval image [50], (b) Re-ranking Top-K retrievals based on the number of inliers [9], (c) Matching all gallery images followed by most inliers sorting [21], (d) Directly performs pixel matching between the UAV image and the reference map without retrieval [53].

Localization Metric: The localization accuracy is denoted as $A@T = \frac{N_T}{N} \times 100\%$, which means the correct localization ratio under a given threshold of T meters. The localization error is denoted as $e_i = \sqrt{(x_p - x_g)^2 + (y_p - y_g)^2}$, where (x_p, y_p) and (x_g, y_g) are the UTM coordinates of predict location and the ground truth, respectively.

Retrieval Metric: The Recall@K and our proposed Pixel Distance Metric (PDM@K, see Eq. (1)) are used. In Eq. (1), R_i denotes the overlap rate between retrievals and the ground truth, $R_i = d_i / (w_i \cdot r)$, where d_i is the spatial distance, w_i is the width of the gallery image, and r is the spatial resolution of the reference map. $\frac{e^{-\lambda \cdot (R_i - \alpha)}}{1 + e^{-\lambda \cdot (R_i - \alpha)}}$ is the retrieval score of the i -th sample in the retrieval result order and $(K - i + 1)$ is the weight. λ and α are weight factors. In this paper, λ is set to 6 and α is set to 0.9. A larger value of PDM@K indicates a better retrieval performance. The rationale of this metric is detailed in Sec. 5.2.

$$PDM@K = \sum_{i=1}^K \frac{(K-i+1) \cdot e^{-\lambda \cdot (R_i - \alpha)}}{1 + e^{-\lambda \cdot (R_i - \alpha)}} / \sum_{i=1}^K (K - i + 1) \quad (1)$$

⁹LPN[42], MCCG[36], Sample4Geo[15] and RK-Net[27]

¹⁰FSRA[12], DenseUAV[13], DAC[47] and CAMP[45]

¹¹D2Net[16], ALIKE[54], Superpoint[14], Superglue[34], Lightglue[28], OmniGlue[25], Xfeat*[33], Key2subpixel[26]

¹²LOFTR[39], RoMa[19], DKM[17] and DeDoDe[18]

Implementation Details: Our experiments were conducted on a machine equipped with Intel Core i9-10920X CPU @ 3.50GHz (128G RAM) and NVIDIA RTX 3090 GPU(24G). For deep learning-based image retrieval approaches, we use the weight trained on the University-1652 dataset[55] with an image size of 384×384 . For deep learning-based image matching approaches, we adopted weights and input sizes from existing works to leverage the models’ optimal performance while testing their generalization capabilities. For NCC and MI, we employed our own implementations. For SIFT, ORB and PnP solver, we used OpenCV implementations. Notably, we use the UAV’s altitude and pitch/yaw information to roughly estimate the image’s scale and rotation, which helps to narrow the search space. Further discussion on this setup is in Sec. 6.3.

5. Experiments on AVL Framework

Based on the unified AVL framework, the state-of-the-art image retrieval and image matching approaches as well as different localization strategies are evaluated in Sec. 5.1, Sec. 5.3 and Sec. 5.4, respectively. 10% of the UAV images and the aerial map are used to do these experiments. Then, the best combined method is selected as the baseline to test the full dataset in Sec. 5.5. Additionally, the analysis of our proposed PDM@K metric is provided in Sec. 5.2.

5.1. Image retrieval Approach

Table 2. Performance Metrics of Retrieval Approaches

Method	R@1	R@3	R@5	P@1	P@3	P@5	ms/feat
NCC[40]	0.3	1.5	2.6	0.157	0.153	0.153	17†
MI[52]	2.4	5.9	8.6	0.303	0.284	0.274	20†
NetVLAD[2]	31.1	53.9	64.9	0.707	0.652	0.604	11
RK-Net[27]	45.3	67.8	76.1	0.817	0.732	0.662	9
LPN[42]	41.1	62.1	70.4	0.769	0.678	0.618	5
FSRA[12]	52.9	73.9	81.2	0.842	0.740	0.671	5
DenseUAV[13]	51.6	69.4	76.7	0.828	0.714	0.639	6
MCCG[36]	56.7	80.5	88.6	0.877	0.799	0.720	6
Sample4Geo[15]	<u>58.6</u>	79.9	86.4	<u>0.882</u>	0.787	0.715	13
DAC[47]	58.3	78.6	84.4	0.874	0.769	0.688	8
CAMP[45]	62.4	82.7	88.3	0.897	0.804	0.722	6

This section aims to identify the best retrieval approaches. As shown in Tab. 2, the handcrafted template matching approaches, NCC and MI, perform worst since they are sensitive to viewpoint difference.

Among deep learning methods, models like CAMP, Sample4Geo, DAC, and MCCG which use ConvNeXt [29] as the backbone achieved better performance: MCCG optimizes network structure for better feature representation, while Sample4Geo, DAC and CAMP focus on the improvements of training and sample strategies, which reveals that training and sampling strategies are more effective for improving the accuracy of current image retrieval models.

Although DenseUAV proposed a new baseline for AVL, it underperformed in multi-view conditions, possibly because the model was mainly designed for nadir-view images. Overall, drone-to-ortho reference map retrieval under Low-altitude, Multi-view condition is still challenging.

To analyze the impact of retrieval accuracy on the subsequent localization accuracy, we also combined retrieval approaches with different matching approaches (SP+LG and Roma) and different localization strategies (Top1 Matching and Top5 Re-rank based on the number of inliers).

From Tab. 3, we can observe that CAMP achieves the highest localization accuracy. This is consistent with the trend observed in Tab. 2.

5.2. Image Retrieval Metric

In UAV AVL tasks, reference maps are geographically continuous, yet Recall@K solely focuses on the result with minimal localization error, disregarding the distribution of other images within Top K. As shown in Fig. 4a, Recall@1 assigns a binary score (1 or 0) to retrieval results, which fails to account for the spatial distribution of retrievals. For instance, in Fig. 5, the 4th ranked image, despite its distance from the ground truth, effectively matches the UAV image with a localization error of 3.8m. Therefore, it is unreasonable for Recall@K to assign this result a score of 0.

The Spatial Distance Metric[13] (SDM@K, see Eq. (2)) partially addresses this issue by considering the spatial distribution of retrieval results. However, SDM@K relies on the spatial distance d_i between the ground truth and the closest retrievals, making it sensitive to variations in the spatial resolution of reference maps. This leads to inconsistent score curves across different maps (see Fig. 4a), which is unfair for evaluation. In contrast, PDM@K normalizes both the image size and spatial resolution with $R_i = d_i / (w_i \cdot r)$, ensuring a fair evaluation across diverse regions’ reference maps.

$$SDM@K = \sum_{i=1}^K \frac{(K-i+1)}{e^{s \cdot d_i}} / \sum_{i=1}^K (K-i+1) \quad (2)$$

Moreover, PDM@K effectively bridges image retrieval accuracy with final localization accuracy. As illustrated in Fig. 5, R_i is correlated with the distance between the retrieved position and ground truth, reflecting the overlap rate of image pairs for subsequent image matching-based localization. Higher R_i indicates lower overlap, increasing image matching difficulty and reducing localization accuracy. For example, in Fig. 5, the first retrieval with $R_i = 0.27$ achieves an error of 1.4m, while the second retrieval with $R_i = 0.35$ has an error of 2.1m. In contrast, the third retrieval with $R_i = 1.37$ leads to localization failure, with an error of 649m due to insufficient overlap. This trend is further supported by the experimental localization accuracy distribution presented in Fig. 4c.

Table 3. Localization Results of Different Image Retrieval Approaches.

Method	Top1 + SP_LG			Top1 + Roma			Top5 Re-rank + SP_LG			Top5 Re-rank + Roma		
	A@5m	A@10m	A@20m	A@5m	A@10m	A@20m	A@5m	A@10m	A@20m	A@5m	A@10m	A@20m
NCC[40]	7.5	9.8	11.4	10.8	13.3	15.2	16.5	22.1	26.2	22.4	28.3	31.4
MI[52]	13.6	18.6	21.4	18.3	21.7	25.4	28.9	38.8	45.0	36.4	44.6	49.7
NetVLAD[2]	41.7	55.3	62.8	49.3	60.0	65.1	55.0	72.1	80.7	64.3	76.6	82.9
RK-Net[27]	49.9	66.6	76.2	62.2	73.9	79.4	60.0	77.5	87.2	68.6	82.6	89.1
LPN[42]	43.6	57.3	66.5	54.1	64.2	69.5	57.1	75.0	84.6	66.8	80.5	86.4
FSRA[12]	51.6	69.3	79.4	64.9	76.7	82.2	60.7	80.5	90.4	71.7	84.9	91.7
DenseUAV[13]	49.7	66.5	76.4	61.7	72.9	79.8	59.0	78.2	88.1	70.3	84.2	90.6
MCCG[36]	54.9	74.2	83.6	68.2	81.4	87.4	63.1	82.1	91.9	72.7	86.2	92.8
Sample4Geo[15]	54.1	72.8	83.2	66.9	78.8	85.7	62.4	82.4	91.9	73.2	87.5	93.7
DAC[47]	53.4	71.3	81.7	66.9	78.8	85.1	62.2	81.8	91.6	72.7	86.9	93.0
CAMP[45]	55.8	75.0	85.1	70.1	81.3	87.6	62.4	82.2	92.4	74.6	87.6	94.2

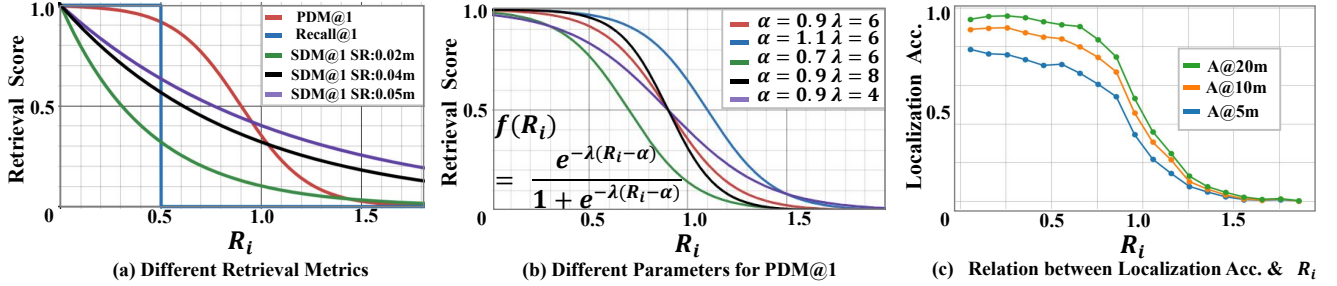


Figure 4. **Illustration of PDM@K.** (a) Different retrieval metric comparison. For clarity in the same figure, we have converted the spatial distance d_i of SDM@1 to R_i and the threshold for Recall@1 is set to 0.5. (b) Different parameter combinations for PDM@1. (c) Relation between localization accuracy and R_i . This curve is based on the actual AVL experiment results.

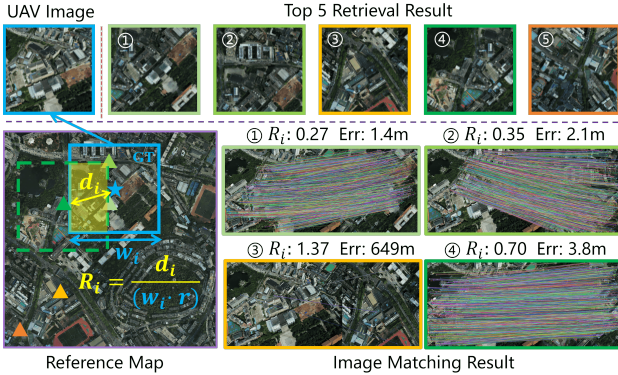


Figure 5. **Visualization of the relation between R_i in PDM@K and subsequent localization accuracy.**

For the retrieval score function $f(R_i)$ (see Fig. 4b), α determines the R_i threshold at which the score drops, while λ controls the sharpness of the decay. When R_i exceeds the normalized diagonal length of the image, l (e.g., $l = 1.67$ when the aspect ratio of drone image is 4:3), there is no overlap between the images, resulting in a score of 0. Therefore, α should be set slightly above $l/2$, and λ can be adjusted based on the impact of different overlap rates on

matching accuracy. On the AnyVisLoc dataset, λ is recommended to be in the range of 4 to 8.

5.3. Image Matching Approach

To evaluate various image matching approaches, we conducted test using CAMP and 12 matching methods. As shown in Tab. 4, learning-based models generally outperform traditional handcrafted methods like SIFT and ORB. While ORB is fast and widely used in SLAM[6], it struggles with significant viewpoint changes. Additionally, Roma excels in dense matching methods, whereas SP+LG_{GIM}+k2s leads in sparse matching. Overall, dense methods significantly surpass sparse methods in localization accuracy, but they suffer from low computational efficiency (e.g., Roma takes over six times longer than SP+LG_{GIM}+k2s). Although DeDoDe attempts to address this issue, it have not achieved good trade-off in our test. Therefore, for real-time localization tasks, sparse matching approaches are more advantageous.

5.4. Localization Strategy

This section compares four distinct localization strategies, the performance metrics are shown in Tab. 5. The retrieval method employed was CAMP, and the matching method was SP+LG_{GIM}+k2s.

Table 4. Localization Results of Different Image Matching Approaches. † denotes the approaches that run on CPU.

Image Matching Method	Top1 + CAMP					Top5 Re-rank + CAMP					Run Time
	A@5m	A@7m	A@10m	A@15m	A@20m	A@5m	A@7m	A@10m	A@15m	A@20m	ms/frame
SIFT[30]	43.9	50.1	55.7	59.9	62.5	52.5	59.4	64.5	68.4	70.8	316†
ORB[6]	3.9	5.8	8.0	10.9	13.6	5.4	7.6	10.3	13.8	17.2	44†
D2Net[16]	27.3	38.1	51.6	61.9	68.6	33.0	44.3	59.8	72.2	78.5	4083
ALIKE[54]	27.7	32.0	34.8	38.2	39.6	31.9	37.3	40.8	44.4	45.9	268
Xfeat*[33]	35.2	44.5	54.4	62.1	66.8	42.8	53.4	63.5	70.7	75.4	69
SP[14]+SG[34]	52.1	63.3	71.7	77.8	80.9	59.1	71.3	79.6	85.8	89.6	92
SP[14]+SG[34]+Omni[25]	45.3	55.0	64.2	72.3	76.1	52.2	63.6	72.9	81.3	84.8	3116†
SP[14]+LG _{GIM} [28, 37]	55.8	66.7	75.0	81.6	85.1	62.4	73.5	82.2	88.9	92.4	75
SP[14]+LG _{GIM} [28, 37]+k2s[26]	57.0	67.6	75.4	81.7	84.8	62.9	74.8	83.2	89.2	91.8	105
LOFTR _{GIM} [37, 39]	59.5	67.4	74.1	79.1	81.6	65.9	74.9	82.5	87.2	89.1	165
DeDoDe[18]	51.5	61.8	69.1	74.8	77.2	61.3	71.6	79.0	84.4	86.9	291
DKM _{GIM} [17, 37]	65.6	73.8	80.2	84.0	86.4	68.5	78.1	85.0	90.3	92.1	4915
Roma[19]	70.1	76.1	81.3	85.7	87.6	73.9	80.8	87.2	91.5	94.0	659

Table 5. Performance Metrics of Localization Strategies

Strategy	A@5m	A@10m	A@20m	s/frame	storage
Matching-wo-Retrieval[53]	34.3	45.7	54.3	1.4	Large
Top1 Matching[50]	55.8	74.3	84.0	0.3	medium
Top5 Re-rank (N=5)[9]	62.2	82.4	91.5	0.8	medium
Most Inliers[21]	64.0	83.2	92.6	10.2	small

The **Direct Matching without Retrieval** strategy performed the worst. In UAV AVL tasks, the area of the reference map (e.g., $9km^2$) is often much larger than the area of the UAV image (e.g., $0.04km^2$). This discrepancy leads to redundant areas in the reference map, which greatly expands the search space of the matching algorithm and result in poor localization robustness.

The **Top1 Matching** strategy uses image retrieval to narrow the search space for subsequent image matching. However, due to the insufficient accuracy of existing image retrieval networks, when the Top1 image is not the ground truth, the subsequent matching algorithm will fail.

The **Top N Re-rank** strategy re-ranks the Top N retrievals based on the number of inliers. The basic assumption is that images with more inliers are often closer to the ground truth and are more suitable for PnP problem solving. Compared to the Top1 strategy, this strategy significantly enhances accuracy with an acceptable increase in time.

The **Most Inliers** strategy directly matches the UAV image with all gallery images and also uses the number of inliers to sort retrievals. Although it has slightly higher localization accuracy than the Top N Re-Rank strategy, feature matching for each gallery image is very time-consuming, making it unable to meet real-time requirements.

Overall, **Top N Re-rank** strategy has a comprehensive advantage in localization accuracy, computation time, and memory usage.

5.5. The Best Combined Method: Baseline

Based on the above experiments, the best combined method which consists of **CAMP+Roma+Top N Rerank** was chosen as the baseline. This baseline was used to test all data in the AnyVisLoc dataset, with results shown in Tab. 6. Although the baseline showed good accuracy at 94.2% within 20 meters (on the aerial map), it only achieved **74.1%** accuracy within 5 meters, which may not meet the precise AVL requirements under low-altitude, multi-view conditions.

Table 6. Performance Metrics for Different Reference Maps

Map	Spatial Resolution(Avg.)		Retrieval Acc.		Localization Acc.		
	2D-Reference	DSM	R@1	P@1	A@5m	A@10m	A@20m
Aerial	0.070m	0.947m	61.6	0.922	74.1	87.7	94.2
Satellite	0.197m	30m	42.8	0.814	18.5	38.7	58.5

6. Factors Affecting the Baseline Accuracy

This section discussed the main factors influencing the localization performance of current baseline. The full dataset is used to conduct the experiment.

6.1. Reference Map

Different reference maps witness different characteristics and localization accuracy (see Tab. 6). **Satellite maps** are easier to obtain but significantly less accurate for localization. This mainly caused by two factors: Firstly, satellite maps have lower spatial resolution, especially with DSM data at 30m. Under Low-altitude Multi-view observation condition, substantial elevation differences in UAV images (e.g., rooftops vs. flat ground) require high-resolution DSM data (e.g. $< 1m$) to ensure accurate PnP problem solving. Secondly, the significant temporal and modality differences between UAV and satellite images pose greater challenges for image retrieval and matching (see Fig. 6c).

Aerial maps provide superior localization accuracy,

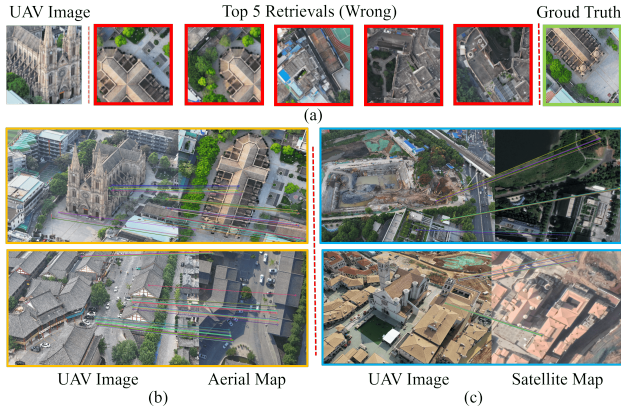


Figure 6. **Challenging Cases for UAV AVL.** The Low-altitude Multi-view condition presents greater challenge for image retrieval (a) and image matching (b). Temporal and modality differences in satellite maps makes localization more difficult (c).

however, pre-aerial photography and precise 3D modeling of the flight area are required, making them less suitable for time-sensitive missions (e.g., emergency rescue) or long-distance flight tasks. Consequently, the choice of reference map type should be tailored to the specific requirements of the mission at hand.

To better analyze the impact of other factors, following experiments are conducted based on the aerial map.

6.2. Multi-view Observation

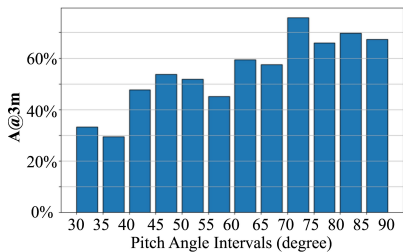


Figure 7. **Impact of Pitch Angle on Localization Accuracy.** A smaller pitch angle tends to reduce localization accuracy.

This section analyzed the localization results across different pitch angles. As shown in Fig. 7, smaller pitch angle tends to reduce localization accuracy, indicating that oblique-view images present greater challenges for accurate localization compared to nadir-view images. In Low-altitude flights, **Oblique-view** images capture substantial side-view information from 3D objects. These interference of side-view details reduces both global and local similarity between UAV images and the ortho-reference map. Consequently, the accuracy of image retrieval and matching algorithms is diminished (see Fig. 6), making precise localization more difficult.

Table 7. **Impact of Different Prior Information Noise on the Localization Accuracy.** Std: standard deviation.

Yaw Std	A@5m	A@10m	A@20m	Pitch Std	A@5m	A@10m	A@20m
0°	74.6	87.6	94.2	0°	74.6	87.6	94.2
5°	74.3(↓ 0.3)	86.3	93.2	3°	73.9(↓ 0.7)	87.2	94.2
10°	72.7(↓ 1.9)	86.4	92.8	5°	73.9(↓ 0.7)	87.1	93.2
20°	72.4(↓ 2.2)	86.4	93.6	7°	73.3(↓ 1.3)	87.3	93.4
30°	70.5(↓ 4.1)	83.5	90.2	10°	72.1(↓ 2.5)	86.5	92.2
50°	60.9(↓ 13.7)	72.8	79.5	20°	71.6(↓ 3.0)	86.2	92.9
60°	48.9(↓ 25.7)	63.0	70.0	30°	69.7(↓ 4.9)	83.7	90.4

(a) Yaw Noise

(b) Pitch Noise

6.3. Noise in Prior Information

Current UAV platforms generally carry sensors that can provide information about pitch/yaw angles and altitude (e.g., gyroscopes and altimeters). In this paper, these information are used to align the UAV image and the reference map to the similar rotation and scale, reducing the search space for retrieval and matching. However, in real scenarios, these prior information often contains noise. To analyze this issue, we added different levels of Gaussian noise (mean of 0) to the prior information. The results are shown in Tab. 7.

Yaw noise affects the rotation estimation. When $std > 10^\circ$, the accuracy of existing image retrieval and matching methods is significantly affected. Notably, the larger the std, the more severely the localization accuracy declines. When the std increases to 30° and 60° , A@5m decreases by 4.1% and 25.7%, respectively.

Pitch noise affects the scale estimation in Eq. (3). Low pitch noise ($std < 5^\circ$) has minimal impact on localization accuracy. However, as pitch noise increases ($std > 7^\circ$), the significant scale difference complicates image retrieval and matching, leading to a noticeable drop in accuracy, with A@5m decreasing by 4.9% at $std = 30^\circ$.

$$r = \frac{altitude}{\sin(pitch)} \cdot \tan\left(\frac{FOV}{2}\right) \cdot \frac{1}{\sqrt{(w^2 + h^2)}} \quad (3)$$

Altitude noise also affects scale estimation like pitch, but its impact is small, the details are put in the appendix.

7. Conclusion

This paper benchmarked the UAV AVL task under **Low-altitude Multi-view** observation condition. The **AnyVis-Loc** dataset is constructed to facilitate a comprehensive test. A **unified framework** is introduced to integrate image-level retrieval, pixel-level matching methods, and various localization strategies. Based on this dataset and framework, state-of-the-art AVL approaches are exhaustively evaluated to select the best combined method as the **baseline**. Additionally, key factors affecting the baseline performance are thoroughly discussed. Overall, the baseline method achieved a **74.1%** accuracy within 5 meters, indicating that there is still much progress to be made and our benchmark is promising to drive further innovation in this field.

References

- [1] Interim regulations on the flight management of unmanned aerial vehicles. https://www.gov.cn/zhengce/content/202306/content_6888799.htm, 2023. 2
- [2] Relja Arandjelovic, Petr Gronat, Akihiko Torii, Tomas Pajdla, and Josef Sivic. Netvlad: Cnn architecture for weakly supervised place recognition. In *CVPR*, pages 5297–5307, 2016. 2, 4, 5, 6
- [3] Herbert Bay, Tinne Tuytelaars, and Luc Van Gool. Surf: Speeded up robust features. In *ECCV*, pages 404–417. Springer, 2006. 2
- [4] Gabriele Berton, Riccardo Mereu, Gabriele Trivigno, Carlo Masone, Gabriela Csurka, Torsten Sattler, and Barbara Caputo. Deep visual geo-localization benchmark. In *Proceedings of the IEEE/CVF Conference on Computer Vision and Pattern Recognition*, pages 5396–5407, 2022. 2
- [5] Mollie Bianchi and Timothy D Barfoot. Uav localization using autoencoded satellite images. *IEEE Robotics and Automation Letters*, 6(2):1761–1768, 2021. 1
- [6] Carlos Campos, Richard Elvira, Juan J. Gómez Rodríguez, José M. M. Montiel, and Juan D. Tardós. Orb-slam3: An accurate open-source library for visual, visual-inertial, and multimap slam. *IEEE Transactions on Robotics*, 37(6):1874–1890, 2021. 1, 2, 4, 6, 7
- [7] Yingxiu Chang, Yongqiang Cheng, Umar Manzoor, and John Murray. A review of uav autonomous navigation in gps-denied environments. *Robotics and Autonomous Systems*, page 104533, 2023. 1
- [8] Jiahao Chen, Enhui Zheng, Ming Dai, Yifu Chen, and Yusheng Lu. Os-fpi: A coarse-to-fine one-stream network for uav geo-localization. *IEEE Journal of Selected Topics in Applied Earth Observations and Remote Sensing*, 2024. 2
- [9] Shuxiao Chen, Xiangyu Wu, Mark W Mueller, and Koushil Sreenath. Real-time geo-localization using satellite imagery and topography for unmanned aerial vehicles. In *2021 IEEE/RSJ International Conference on Intelligent Robots and Systems (IROS)*, pages 2275–2281. IEEE, 2021. 4, 7
- [10] Yuan Chen and Jie Jiang. An oblique-robust absolute visual localization method for gps-denied uav with satellite imagery. *IEEE Transactions on Geoscience and Remote Sensing*, 2023. 1, 2, 3
- [11] Andy Couturier and Moulay A Akhloufi. A review on absolute visual localization for uav. *Robotics and Autonomous Systems*, 135:103666, 2021. 1, 3
- [12] Ming Dai, Jianhong Hu, Jiedong Zhuang, and Enhui Zheng. A transformer-based feature segmentation and region alignment method for uav-view geo-localization. *IEEE TCSVT*, 32(7):4376–4389, 2021. 2, 4, 5, 6
- [13] Ming Dai, Enhui Zheng, Zhenhua Feng, Lei Qi, Jiedong Zhuang, and Wankou Yang. Vision-based uav self-positioning in low-altitude urban environments. *IEEE Transactions on Image Processing*, 2023. 1, 2, 3, 4, 5, 6
- [14] Daniel DeTone, Tomasz Malisiewicz, and Andrew Rabinovich. Superpoint: Self-supervised interest point detection and description. In *CVPRw*, 2018. 2, 4, 7
- [15] Fabian Deuser, Konrad Habel, and Norbert Oswald. Sample4geo: Hard negative sampling for cross-view geo-localisation. In *ICCV*, pages 16847–16856, 2023. 2, 4, 5, 6
- [16] Mihai Dusmanu, Ignacio Rocco, Tomas Pajdla, Marc Pollefeys, Josef Sivic, Akihiko Torii, and Torsten Sattler. D2-Net: A Trainable CNN for Joint Detection and Description of Local Features. In *CVPR*, 2019. 2, 4, 7
- [17] Johan Edstedt, Ioannis Athanasiadis, Mårten Wadenbäck, and Michael Felsberg. DKM: Dense kernelized feature matching for geometry estimation. In *CVPR*, 2023. 2, 4, 7
- [18] Johan Edstedt, Georg Bökman, Mårten Wadenbäck, and Michael Felsberg. Dedode: Detect, don’t describe—describe, don’t detect for local feature matching. In *2024 International Conference on 3D Vision (3DV)*, pages 148–157. IEEE, 2024. 4, 7
- [19] Johan Edstedt, Qiyu Sun, Georg Bökman, Mårten Wadenbäck, and Michael Felsberg. RoMa: Robust Dense Feature Matching. *CVPR*, 2024. 2, 4, 7
- [20] Xiao-Shan Gao, Xiao-Rong Hou, Jianliang Tang, and Hang-Fei Cheng. Complete solution classification for the perspective-three-point problem. *IEEE transactions on pattern analysis and machine intelligence*, 25(8):930–943, 2003. 4
- [21] Marius-Mihail Gurgu, Jorge Peña Queraltá, and Tomi West-erlund. Vision-based gnss-free localization for uavs in the wild. In *2022 7th International Conference on Mechanical Engineering and Robotics Research (ICMERR)*, pages 7–12. IEEE, 2022. 2, 3, 4, 7
- [22] Mengfan He, Jiacheng Liu, Pengfei Gu, and Ziyang Meng. Leveraging map retrieval and alignment for robust uav visual geo-localization. *IEEE Transactions on Instrumentation and Measurement*, 2024. 1
- [23] Yao He, Ivan Cisneros, Nikhil Keetha, Jay Patrikar, Zelin Ye, Ian Higgins, Yaoyu Hu, Parv Kapoor, and Sebastian Scherer. Foundloc: Vision-based onboard aerial localization in the wild. *arXiv preprint arXiv:2310.16299*, 2023. 1
- [24] Yuxiang Ji, Boyong He, Zhuoyue Tan, and Liaoni Wu. Game4loc: A uav geo-localization benchmark from game data. In *AAAI*, 2025. 3
- [25] Hanwen Jiang, Arjun Karpur, Bingyi Cao, Qixing Huang, and André Araujo. Omniglu: Generalizable feature matching with foundation model guidance. In *CVPR*, pages 19865–19875, 2024. 2, 4, 7
- [26] Shinjeong Kim, Marc Pollefeys, and Daniel Barath. Learning to make keypoints sub-pixel accurate. In *ECCV*, 2024. 2, 4, 7
- [27] Jinliang Lin, Zhedong Zheng, Zhun Zhong, Zhiming Luo, Shaozi Li, Yi Yang, and Nicu Sebe. Joint representation learning and keypoint detection for cross-view geo-localization. *IEEE Transactions on Image Processing (TIP)*, 2022. 2, 4, 5, 6
- [28] Philipp Lindenberger, Paul-Edouard Sarlin, and Marc Pollefeys. LightGlue: Local Feature Matching at Light Speed. In *ICCV*, 2023. 2, 4, 7
- [29] Zhuang Liu, Hanzi Mao, Chao-Yuan Wu, Christoph Feichtenhofer, Trevor Darrell, and Saining Xie. A convnet for the 2020s. *CVPR*, 2022. 5

- [30] D. G. Lowe. Distinctive image features from scale-invariant keypoints. *Int. J. Comput. Vis.*, 60(2):91–110, 2004. 2, 4, 7
- [31] Xiaoyong Lu and Songlin Du. Raising the ceiling: Conflict-free local feature matching with dynamic view switching. In *ECCV*, pages 256–273. Springer, 2024. 2
- [32] Muhammad Hamza Mughal, Muhammad Jawad Khokhar, and Muhammad Shahzad. Assisting uav localization via deep contextual image matching. *IEEE Journal of Selected Topics in Applied Earth Observations and Remote Sensing*, 14:2445–2457, 2021. 1, 2, 3
- [33] Guilherme Potje, Felipe Cadar, André Araujo, Renato Martins, and Erickson R Nascimento. Xfeat: Accelerated features for lightweight image matching. In *CVPR*, pages 2682–2691, 2024. 2, 4, 7
- [34] Paul-Edouard Sarlin, Daniel DeTone, Tomasz Malisiewicz, and Andrew Rabinovich. SuperGlue: Learning feature matching with graph neural networks. In *CVPR*, 2020. 2, 4, 7
- [35] Michael Schleiss, Fahmi Rouatbi, and Daniel Cremers. Vpair-aerial visual place recognition and localization in large-scale outdoor environments. *arXiv:2205.11567*, 2022. 1, 3
- [36] Tianrui Shen, Yingmei Wei, Lai Kang, Shanshan Wan, and Yee-Hong Yang. Mccg: A convnext-based multiple-classifier method for cross-view geo-localization. *IEEE TCSVT*, 2023. 2, 4, 5, 6
- [37] Xuelun Shen, Zhipeng Cai, Wei Yin, Matthias Müller, Zijun Li, Kaixuan Wang, Xiaozhi Chen, and Cheng Wang. Gim: Learning generalizable image matcher from internet videos. In *ICLR*, 2024. 7
- [38] Woo-Hyuck Song, Hong-Gyu Jung, In-Youb Gwak, and Seong-Whan Lee. Oblique aerial image matching based on iterative simulation and homography evaluation. *Pattern Recognition*, 87:317–331, 2019. 2, 3
- [39] Jiaming Sun, Zehong Shen, Yuang Wang, Hujun Bao, and Xiaowei Zhou. Loftr: Detector-free local feature matching with transformers. In *CVPR*, 2021. 2, 4, 7
- [40] Gerald J Van Dalen, Daniel P Magree, and Eric N Johnson. Absolute localization using image alignment and particle filtering. In *AIAA Guidance, Navigation, and Control Conference*, page 0647, 2016. 2, 4, 5, 6
- [41] Chengyi Wang, Jingbo Chen, Jiansheng Chen, Anzhi Yue, Dongxu He, Qingqing Huang, and Yi Zhang. Unmanned aerial vehicle oblique image registration using an asift-based matching method. *Journal of Applied Remote Sensing*, 12(2):025002–025002, 2018. 3
- [42] Tingyu Wang, Zhedong Zheng, Chenggang Yan, Jiyong Zhang, Yaoqi Sun, Bolun Zheng, and Yi Yang. Each part matters: Local patterns facilitate cross-view geo-localization. *IEEE TCSVT*, 32(2):867–879, 2021. 2, 4, 5, 6
- [43] Yifan Wang, Xingyi He, Sida Peng, Dongli Tan, and Xiaowei Zhou. Efficient loftr: Semi-dense local feature matching with sparse-like speed. In *CVPR*, pages 21666–21675, 2024. 2
- [44] Zhen Wang, Dianxi Shi, Chunping Qiu, Songchang Jin, Tongyue Li, Yanyan Shi, Zhe Liu, and Ziteng Qiao. Sequence matching for image-based uav-to-satellite geolocalization. *IEEE Transactions on Geoscience and Remote Sensing*, 2024. 1
- [45] Qiong Wu, Yi Wan, Zhi Zheng, Yongjun Zhang, Guangshuai Wang, and Zhenyang Zhao. Camp: A cross-view geo-localization method using contrastive attributes mining and position-aware partitioning. *IEEE Transactions on Geoscience and Remote Sensing*, 2024. 2, 4, 5, 6
- [46] Rouwan Wu, Xiaoya Cheng, Juelin Zhu, Xuxiang Liu, Maojun Zhang, and Shen Yan. Uavd4l: A large-scale dataset for uav 6-dof localization. In *International Conference on 3D Vision (3DV)*, 2024. 3
- [47] Panwang Xia, Yi Wan, Zhi Zheng, Yongjun Zhang, and Jiwei Deng. Enhancing cross-view geo-localization with domain alignment and scene consistency. *IEEE TCSVT*, 2024. 2, 4, 5, 6
- [48] Wenjia Xu, Yaxuan Yao, Jiaqi Cao, Zhiwei Wei, Chunbo Liu, Jiuniu Wang, and Mugen Peng. Uav-visloc: A large-scale dataset for uav visual localization. *arXiv preprint arXiv:2405.11936*, 2024. 2, 3
- [49] Nian Xue, Liang Niu, Xianbin Hong, Zhen Li, Larissa Hof-faeller, and Christina Pöpper. DeepSim: Gps spoofing detection on uavs using satellite imagery matching. In *Proceedings of the 36th Annual Computer Security Applications Conference*, page 304–319, New York, NY, USA, 2020. Association for Computing Machinery. 1
- [50] Qin Ye, Junqi Luo, and Yi Lin. A coarse-to-fine visual geo-localization method for gnss-denied uav with oblique-view imagery. *ISPRS Journal of Photogrammetry and Remote Sensing*, 212:306–322, 2024. 2, 3, 4, 7
- [51] Peng Yin, Ivan Cisneros, Shiqi Zhao, Ji Zhang, Howie Choset, and Sebastian Scherer. isimloc: Visual global localization for previously unseen environments with simulated images. *IEEE Transactions on Robotics*, 39(3):1893–1909, 2023. 2
- [52] Aurelien Yol, Bertrand Delabarre, Amaury Dame, Jean-milic Dartois, and Eric Marchand. Vision-based absolute localization for unmanned aerial vehicles. In *2014 IEEE/RSJ International Conference on Intelligent Robots and Systems*, pages 3429–3434. IEEE, 2014. 2, 4, 5, 6
- [53] Yijie Yuan, Wei Huang, Xiangxin Wang, Huaiyu Xu, Hongying Zuo, and Ruidan Su. Automated accurate registration method between uav image and google satellite map. *Multimedia Tools and Applications*, 79:16573–16591, 2020. 4, 7
- [54] Xiaoming Zhao, Xingming Wu, Jinyu Miao, Weihai Chen, Peter CY Chen, and Zhengguo Li. Alike: Accurate and lightweight keypoint detection and descriptor extraction. *IEEE Transactions on Multimedia*, 25:3101–3112, 2022. 2, 4, 7
- [55] Zhedong Zheng, Yunchao Wei, and Yi Yang. University-1652: A multi-view multi-source benchmark for drone-based geo-localization. In *Proceedings of the 28th ACM international conference on Multimedia*, pages 1395–1403, 2020. 2, 3, 5
- [56] Runzhe Zhu, Ling Yin, Mingze Yang, Fei Wu, Yuncheng Yang, and Wenbo Hu. Sues-200: A multi-height multi-scene cross-view image benchmark across drone and satellite. *IEEE TCSVT*, 33(9):4825–4839, 2023. 2, 3